Quantification of Fluid Structure Interaction Dynamics in a Deformable Vocal Fold Model with Injected Materials

Preston R. Murray

Department of Mechanical Engineering, Brigham Young University, Provo, Utah, 84602

The influence of injections on the fluid structure interactions was evaluated on a deformable life sized, synthetic, self-oscillating model with idealized geometry of human vocal folds. Two models were designed to incorporate 10% and 20% bowing similar to that found in patients with vocal fold paralysis. The models were fabricated from a flexible silicone compound with Young's modulus values similar to those found in human vocal folds. The models incorporated a two-layer design that simulated the layered vocal fold structure. The bowed models were paired with "healthy" models and injected with silicone material until the gap from the designed bowing was closed. The effects of the injections were compared by measuring flow rate, frequency, onset pressure (a measure of vocal effort), and maximum glottal gap. High-speed imaging of the superior surface was used to determine qualitative data on the oscillation pattern. Flow rate, onset pressure, and maximum glottal gap were all reduced after injections were placed for both bowing cases. Frequency increased for the 10% bowed case and remained unchanged for the 20% bowed case. Suggestions for future related studies are discussed.

1 INTRODUCTION

Flow-induced vibration (FIV) is classified as the dynamic response of a structure in contact with fluid flow. Applications of this are found in aeronautics (e.g., airfoil flutter and stall flutter that occurs when the flow separates). Other examples of areas in which FIVs are significant include blood flow and associated tissue dynamics, flow around suspension bridges, heat exchangers, and the flow within the vocal tract that results in voice production (Kaneko, et al., 2008; Thomson, et al., 2005). Such fluid-structure interaction (FSI) problems are both important and challenging, because of the inclusion of many strongly coupled, nonlinear factors (Dowell, et al., 2001). These types of interactions are found any time fluid flows around a deformable medium. FSI phenomena are found in tents, parachutes, airbags, and arteries. While much research has been done on the FIV and FSI on standardized geometry such as cylinders and ellipses, relatively little research has been done on the FIV and FSI dynamics of multilayered, viscoelastic, deformable bodies.

The source of sound of the human voice happens in the dynamic gap between the vocal folds. The lungs induce pressure on the vocal folds which separate until the pressure decreases such that structural forces of the vocal folds dominate and close the gap. This process leads to a pulsating air jet from which sound is produced (Van den Berg, 1958).

In order to study this phenomenon, self-oscillating synthetic vocal fold models have been created which incorporate similar FIV and FSI of human vocal folds to create sound. These models have proven useful in investigating various aspects of the voice, including: quantifying impact as the vocal folds collide (Spencer, et al., 2008) , quantification of supraglottal vortices (Neubauer,

1

et al., 2007) , and development of *in-vivo* measurement devices (Popolo, et al., 2008). Synthetic vocal fold models are used because they exhibit life-like characteristics, are repeatable, have life spans of months, and can be parameterized.

Various synthetic self oscillating vocal fold models exist in current research. The "M5" geometry developed by Scherer et. al. (2001) was used for construction of synthetic vocal fold models (Thomson, et al., 2005; Fulcher, et al., 2006; Spencer, et al., 2008; Neubauer, et al., 2007; Popolo, et al., 2008). These models are made from a flexible three part silicone compound that allows for large deformations. These models are of similar size, shape, and material properties of human vocal folds. Advantages of this model include ease of parameterization, durability and it relatively good agreement with human vocal folds. Disadvantages are idealized geometry and incorrect vocal fold motion including prominent vertical motion, minimal convergent/divergent profile (alternating angle of the medial surface), and limited mucosal wave (undulation from inferior to superior portion of the medial surface).

A computational study was performed by Pickup et al. (2011) to incorporate the advantages of the M5 models while improving the medial surface dynamics. By altering the M5 geometry, the dominant geometries were determined that affected maximum glottal width, flow rate, and intraglottal angle. The synthetic self-oscillating two-layer model used in this study was created from the results.

The purpose of this study is to 1) develop a self-oscillating multi-layered synthetic vocal fold model into which a viscoelastic medium can be injected, and 2) quantify the effects of the injection on the vibratory pattern.

2 METHODS

2.1 Self-Oscillating Synthetic Models

The synthetic models used in this study were an alteration of the geometry for a two layer model specified by Pickup et al. (2011) that included bowing to mimic vocal fold paralysis. The bowing was defined as an atrophy of the interior muscle of the vocal fold. By varying the degree of atrophy, a model was created that incorporated a bowing of 10% and 20% from a "healthy" model as shown in Figure 1.
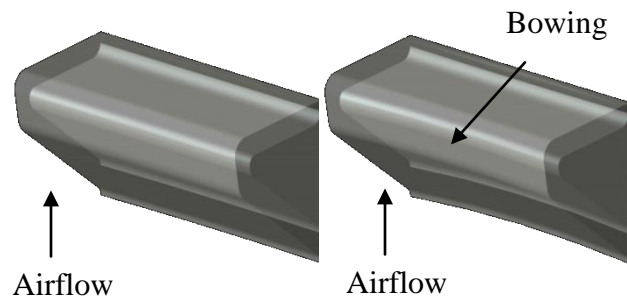

Figure 1 – One side of a pair of vocal folds. The healthy (left) and bowed (right) models are shown. The interior portion is the body; the exterior portion is the cover. Airflow is from low to high.

The two layers of the model had different material properties. The model was created using a three part addition cure silicone rubber (Ecoflex 0030, Smooth-On, Inc.). Variation in stiffness was controlled by adding varying amounts of thinner (more thinner reduces the modulus of the material). Both bowed and "healthy" models were made of the same material properties in each layer. Further details on model fabrication can be found elsewhere (Thomson, 2004; Thomson, et al., 2005; Pickup, et al., 2010).

2.2 Material Properties

Each section of the vocal fold models was created separately enabling the simultaneous fabrication of tensile and rheological test specimens. The tensile specimens were columns 8 mm in diameter and 50 mm long and tested in an

Instron (3342) tensile tester. The testing procedure included a pre-stressing cycle, followed by the testing cycle. In each case, the specimen was elongated to 40% strain. The Young's modulus was measured for each batch of silicone (see Table 1). These values were similar to those used in previous synthetic and computational studies (Alipour et al., 200; Thomson et al., 2005; Drechsel and Thomson, 2008), and of a similar magnitude to the Young's modulus of human vocal fold tissue in the small-strain regime (Chan, et al., 2007).

Table 1 - Modulus for various mixture ratios obtained from tensile tests.

Silicone Mixture	Modulus (kPa)
1:1:4	2.08
1:1:2	3.83
1:1:0.5	11.6

The rheological specimens were disks 40 mm in diameter, 2 mm thick and tested in a Rheometer (AR 2000EX, TA Instruments, Inc.). The specimens were subject to an oscillation cycle ranging from 1 to 100 Hz with the controlled variable being 40% strain in order to determine the storage modulus (G') and the loss modulus (G") (see Figure 2).

It was shown that the storage moduli of the stiffer silicones were relatively flat while the thinner mixtures were flat at lower frequencies and increased at higher frequencies. The loss modulus increased for all samples as angular frequency increased. These properties showed that the materials used in the vocal fold models were viscoelastic.

2.3 Experimental Setup

The experimental setup in Figure 3 allowed the recording of the superior surface. Air flow was supplied by pressurized air connected to a rigid plenum. The flow rate was measured by a rotometer type flow meter (Key Instruments, FR4A37BVBN). A differential pressure transducer (Omega PXI 138-001D5V), mounted approximately 3 cm upstream of the model, measured the subglottal pressure. A high-speed digital camera (Photron SA3) using a 50 mm lens
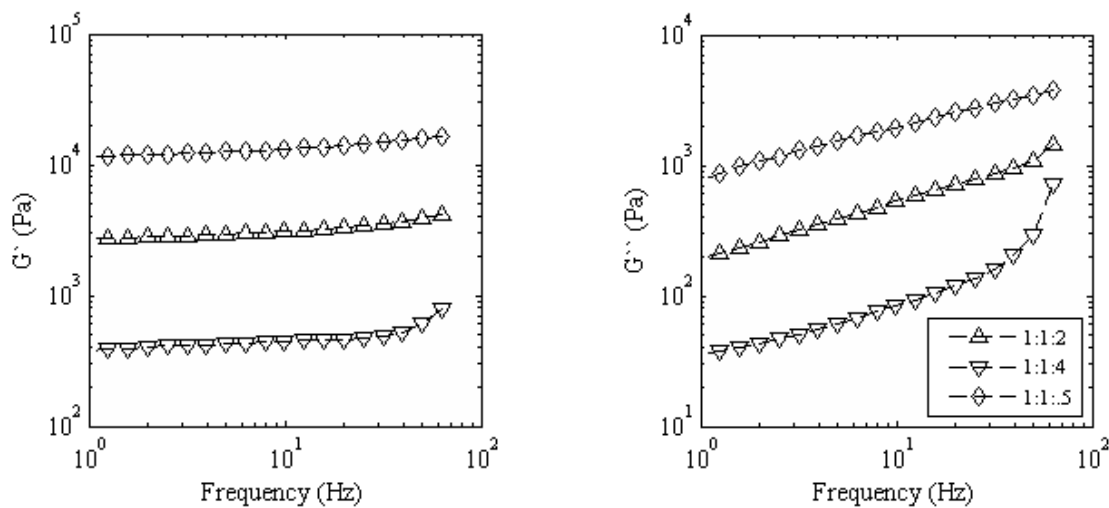

Figure 2 – Storage (left) and loss (right) moduli of the materials used in the vocal fold models.

(AF Nikkor) and a 12 mm extension ring (AF Zeikos Macro) at 3,000 fps and 1/6,000 shutter speed shutter speed captured the model motion from a superior view. Four LED lights were used for illumination (Visual Instrumentation Corporation 900415). Air pressure was applied and the onset pressure (pressure at which vibration begins) was determined through multiple tests. The air pressure for the imaging was set at 110%, 120% and 130% of the measured onset pressure. Frequency was found using a data acquisition system (PXI-1042Q) and custom LabVIEW programming. Each vocal fold model pair placed on the plate was calibrated using a ruler placed in the image. The high speed images of the superior surface were processed using custom Matlab code that identified the edge of the vocal fold models using grayscale intensity thresholding, from which the maximum glottal gap (gap between vocal fold models) was extracted. Each bowed model was paired with a "healthy" model.

The injections were placed using a 22 gage 1.5 inch needle (Beckton Dickenson, 305156) and 500 μl syringe (Hamilton 81220). The vocal fold was penetrated through the tough
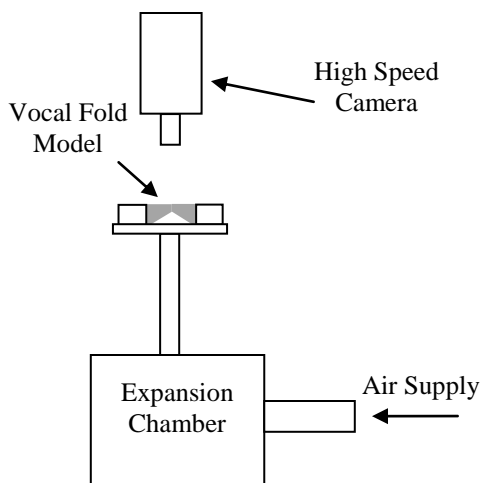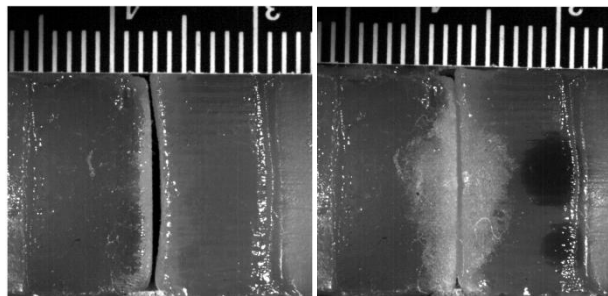

Figure 3 – Experimental setup for visualizing the superior surface of the vocal fold models.
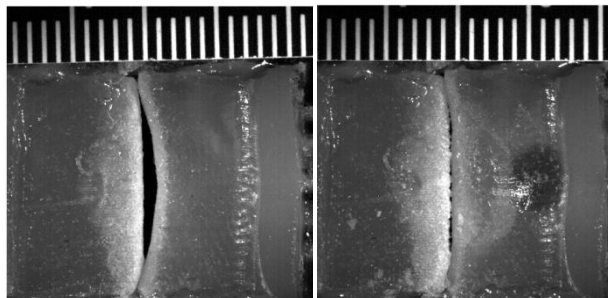
10% Bowed Case

20% Bowed Case

Figure 4 – Superior view of the pre- (left) and post- (right) injection for the two cases. In each picture, the left and right vocal fold models were the "healthy" and bowed models, respectively. The dark circle was the injection. The ruler enabled calibration.

support material and the injection placed immediately on the other side. Figure 4 shows before and after injection results for both models.

For each model, the onset pressure was determined by increasing the subglottal pressure until vibration began. This process was repeated five times and the average and standard deviation were determined (see Table 2). For comparison purposes, each model was vibrated at 110%, 120%, and 130% of its onset pressure and its frequency, maximum glottal width and flow rate were compared.

Table 2 – Mean and standard deviation (in parentheses) of onset pressures pre- and post-injection.

Model	Onset Pressure (kPa)	
	Pre-Injection	**Post-Injection**
10% Bowing	1.00 (0.008)	0.86 (0.019)
20% Bowing	1.57 (0.034)	1.53 (0.019)

3   RESULTS AND DISCUSSION

3.1   Flow Rate

The flow rate results from the experiment are found in Figure 5. It was determined that the 20% bowing had approximately twice the flow rate as the model with 10% bowing. For the 10% bowing model, the flow rate was reduced by approximately 37% while the reduction in the model with 20% bowing was 14%. The onset pressure decreased by 17% for the 10% bowing case, and 2.4% for the 20% bowed case. The direction of inflection of the curves for both models changed after the fluid was injected.

Doellinger et at. (2006) reported flow rates for excised larynges between 200 and 400 ml/s. For both cases, even after the injections, the flow rates were well above normal values.
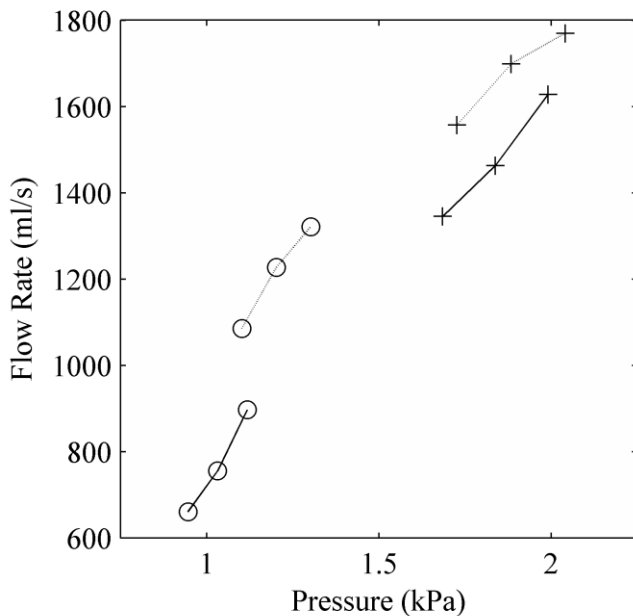

Figure 5 - Volumetric flow rate versus pressure. Circles and plus signs are 10% and 20 percent bowing respectively. Dashed lines are pre-injection and solid lines are post-injection.
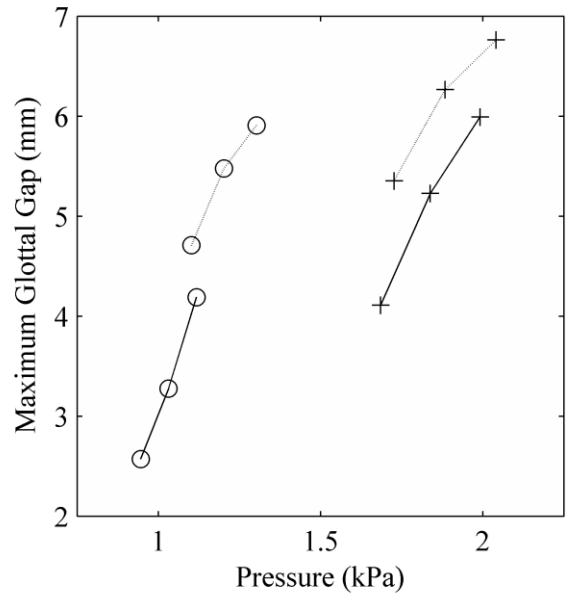
3.2   Maximum Glottal Gap

Figure 6 - Maximum glottal gap versus pressure. Circles and plus signs are 10% and 20 percent bowing respectively. Dashed lines are pre-injection and solid lines are post-injection.

The maximum glottal gap results are shown Figure 6. Similar trends were present in the maximum glottal gap compared to the results from flow rate. This showed that the injection was successful in closing the glottal gap with and without inducing vibration.

3.3   Fundamental Frequency

The effect of the injections on the fundamental frequency showed a small decrease for the 20% bowed model, however, there was an inverse effect for the 10% bowed model. This result showed for the 10% bowed case there was a stiffening of the model as more material was introduced. Although there was more material injected into the model with 20% bowing, the fundamental frequency did not change appreciably.
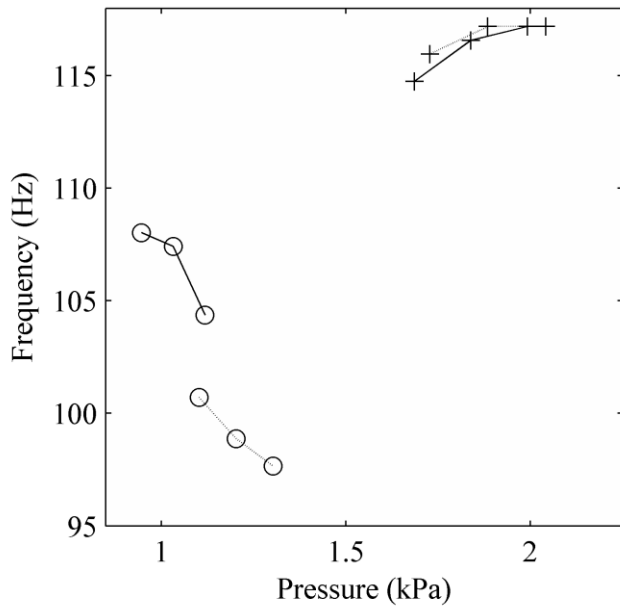
Figure 7 – Fundamental frequency versus pressure. Circles and plus signs are 10% and 20 percent bowing respectively. Dashed lines are pre-injection and solid lines are post-injection.

3.4 Superior High Speed Images

Superior views of one period of oscillation for both model types pre- and post-injection are shown in Figure 8. In all cases the models were vibrating at 120% of their respective onset pressures. There was slight asymmetry in the 10% bowed before injections and less post-injection. In contrast, the 20% bowed case showed extreme asymmetry pre-injection which was slightly mitigated after the injection was placed. This showed that although more material was injected into the 20% bowed case, it did not have as substantial of an effect on glottal closure or asymmetry as the 10% bowed case. Also, none of the models show complete closure which resulted in a low quality "breathy" sound.
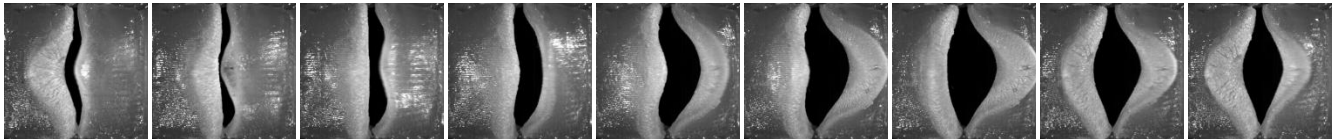
10% Bowing Pre-Injection
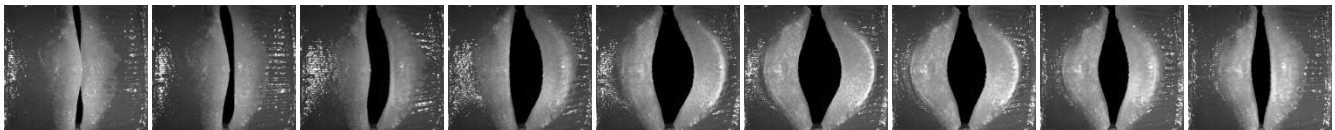
10% Bowing Post-Injection
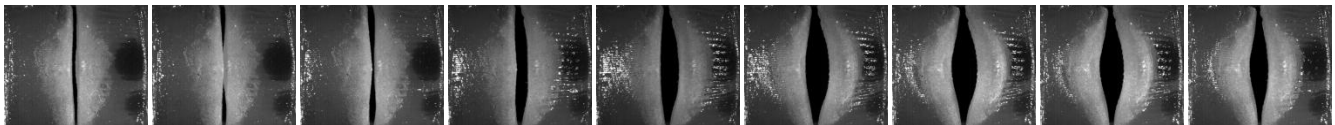
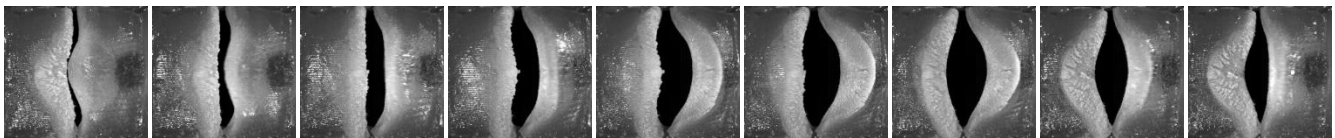20% Bowing Pre-Injection

20% Bowing Post-Injection

Figure 8 - Timeline of one period of oscillation for both models pre- and post-injection. In all pictures the bowed model is on the right and the "healthy" model is on the left. Dark spots are present in the bowed models post-injection

4 CONCLUSIONS

Vocal fold models were designed and built that incorporated 10% and 20% bowing. These models were paired with a "healthy" model and flow rate, maximum glottal gap, and frequency pre- and post-injection were obtained and compared. High speed images of one period of oscillation of the superior surface were also compared. Material was injected into the vocal fold models until the gap between the models was closed. Injecting material decreased the onset pressure, flow rate, and maximum glottal gap for both the 10% and 20% bowed cases. However, the frequency for the 10% bowed case increased while change in the frequency for the 20% case was negligible. The high speed images of the superior surface showed asymmetry in the pre- injection oscillations for both models. The asymmetry for the 10% case was mitigated after injection while asymmetry for the 20% bowed case remained present.

Two areas of future work are recommended. First, injections were placed mainly in the center of the models until the gap between the vocal fold models closed. While this was effective at alleviating asymmetry in the 10% bowed model, the same process had little effect on the asymmetry of the model with 20% bowing. An investigation into why this occurred would allow a further understanding of the effect of injections on more drastically bowed vocal folds. Second, injections were placed only until the gap closed. An investigation on the effects of over-injecting the vocal fold models would determine the effects of introducing unnecessary injected material into the models. Finally, a study that incorporates injections in multiple locations in order to close the glottal gap would facilitate the understanding of the effects of injecting material in various locations.

6 REFERENCES

Aliour, F., Berry, D. A., & Titze, I. R. (2000). A finite-element model of vocal-fold vibration. *Journal of the Acoustical Society of America , 108* (6), 3003-3012.

Chan, R. W., Fu, M., Young, L., & Tirunagari, N. (2007). Relative contributions of collagen and elastin to elasticity of the vocal fold under tension. *Annals of Biomedical Engineering , 35* (8), 1471-1483.

Dowell, E. H., & Hall, K. C. (2001). Modeling of fluid structure interaction. *Annual Review of Fluid Mechanics , 33*, 445-490.

Drechsel, J. S., & Thomson, S. L. (2008). Influence of supraglottal structures on the glottal jet exiting a two-layer synthetic, self-oscillating vocal fold model. *Journal of the Acoustical Society of America , 123* (6), 4434-4445.

Fulcher, L. P., Scherer, R. C., Zhai, G., & Zhu, Z. (2006). Analytic representation of volume flow as a function of geometry and pressure in a static physical model of the glottis. *Journal of Voice , 20*, 489-512.

Hirano, M., & Kakita, Y. (1985). Cover body theory of vocal fold vibration. In R. G. Daniloff (Ed.), *Speech Science* (pp. 1-46). San Diego, CA: College-Hill Press.

Kaneko, S., Nakamura, T., Inada, F., & Kato, M. (2008). *Flow-induced vibrations: Classifications and lessons from practical experiences.* Oxford, UK: Charon Tec Ltd.

Neubauer, J., Zhang, Z., Miraghaio, R., & Berry, D. A. (2007). Coherent structures of the near field flow in a self-oscillating physical model of the vocal folds. *Journal of the Acoustical Society of America , 121* (2), 1102-1118.

Pickup, B. A., & Thomson, S. L. (2010). Flow-induced vibratory response of idealized versus magnetic resonance imaging-based synthetic vocal fold models. *Journal of the Acoustical Society of America , 128* (3).

Pickup, B. A., & Thomson, S. L. (2011). Identification of geometric parameters influencing the flow-induced vibration of a two-layer self-oscillating computational vocal fold model. *Journal of the Acoustical Society of America , 129* (4), 2121-2132.

Popolo, P. S., & Titze, I. R. (2008). Qualification of a quantitative laryngeal imaging system using videostroboscopy and videokymography. *Annals of Otology, Rhinology & Laryngology , 117* (6), 4014-412.

Scherer, R., Shinwari, D., De Witt, K., Zhang, C., Kucinschi, B., & Afjeh, A. (2001). Intraglottal pressure profiles for a symmetric and oblique glottis with a divergence angle of 10 degrees. *Journal of the Acoustical Society of America , 109*, 1616-1630.

Spencer, M., Siegmund, T., & Mongeau, L. (2008). Determination of superior surface strains and stresses, and vocal fold contact pressure in a synthetic larynx model using digital image correlation. *Journal of the Acoustical Society of America , 123* (2), 1089-1103.

Thomson, S. (2004). Fluid-structure interactions within the human larynx, Ph.D. dissertation. West Lafayette, Indiana.

Thomson, S. L., Mongeau, L., & Frankel, S. H. (2005). Aerodynamic transfer of energy to the vocal folds. *Journal of the Acoustical Society of America , 118*, 1689-1700.

Van den Berg, J. (1958). Myoelastic-aerodynamic theory of voice production. *Journal of Speech and Hearing Research , 1*, 227-244.